

THEORY OF THE NEAR-PROBE LAYER IN ELECTRONEGATIVE GASES

S. A. Gutsev

UDC 537

Experimental data on an investigation of a plasma, containing negative ions, in the active discharge phase and in the afterglow stage are reported. The applicability of the orbital-motion theory to probe investigations in electronegative gases is discussed.

Works concerned with a low-temperature plasma that contains negative ions have appeared recently in the scientific literature. In the overwhelming majority of these works, the main method of diagnostics is investigations using electrical probes. As is known, probe diagnostics makes it possible to obtain information about local characteristics of a plasma. On the other hand, in the literature one can find diametrically opposite data on the processes occurring in a plasma and its parameters. This indicates that the procedure of measurements in a plasma of electronegative gases is insufficiently developed. In our opinion, the least studied aspect is the influence of the probe and its electric field on the plasma properties and the parameters determined.

As the object of the present investigation, we chose a pulsed-discharge oxygen plasma. The gas pressure was 0.07 torr, the pulse frequency was 1.5 kHz, and the relative pulse spacing was 10. The discharge was initiated in a cylindrical tube with a radius of 1.75 cm and a length of 40 cm; the pulse current was 80 mA. Measurements were performed with the aid of two sliding molybdenum probes with a length of 1.5 and 0.35 cm, whose radii were 0.01 and 0.005 cm, respectively. For diagnostics, a measuring unit was manufactured that allowed the recording of volt-ampere characteristics (VAC) and their second derivatives in the active discharge phase and in the afterglow stage. Figure 1 shows the radial dependence of VAC measured in the active discharge phase by the probe with a length of 1.5 cm and a radius of 0.01 cm. As is seen, the characteristics have no saturation current of the negative particles. The electron temperature, measured by the method of taking the logarithm of the steep part of the VAC, was 1.96 eV. We failed to measure the second derivative (by the method of modulation of the second harmonic) because of the high level of noise in the active discharge phase. The estimated mean free path of the electrons in the collision cross section [1] was 1.3 cm. The magnitude of the electric field of the positive column measured between two probes was 3 V/cm. The electron concentration estimated by the magnitudes of the current, electric field, and electron mobility [2] was $6 \cdot 10^9 \text{ cm}^{-3}$.

Since the VAC has no saturation current of the negative particles, we can presume that, under the given discharge conditions, the mode of orbital motion (OML) of the charged particles toward the probe is implemented. According to the OML theory for a cylindrical probe, the plot of $I^2(U)$ in the region $kT \gg eU$ is a straight line. Figure 2 shows plots of $I^2(U)$ constructed from Fig. 1. The main contribution to the current of negative particles is made by electrons; the current of negative ions can be neglected. In the region $kT \gg eU$, the experimental values of $I_e^2(U)$ coincide with straight lines; their asymptotic form crosses the axis of potentials at one point, i.e., the electron temperature is practically the same over the tube radius. The electron concentration was determined from the slope of $I_e^2(U)$ [3] and along the tube axis it was $8.2 \cdot 10^9 \text{ cm}^{-3}$, which agrees well with the estimated value given above. The radial profile of the electron density is shown in Fig. 3. It is seen that in the near-wall region it is substantially steeper than a Bessel distribution.

St. Petersburg Scientific-Research Institute of Physics at the State University, Russia. Translated from *Inzhenerno-Fizicheskii Zhurnal*, Vol. 73, No. 2, pp. 321-327, March-April, 2000. Original article submitted November 5, 1998.

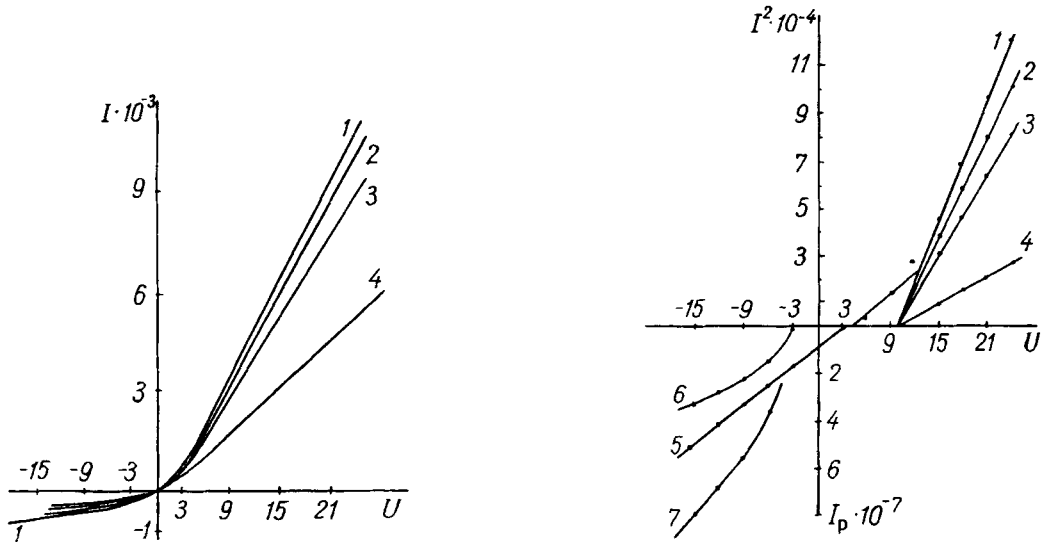


Fig. 1. Radial dependence of the VAC in the active discharge phase: 1) $r = 0$; 2) 0.5; 3) 1.0; 4) 1.5 cm. I , A; U , V.

Fig. 2. Radial dependence of $I^2(U)$ in the active discharge phase: 1) $r = 0$; 2) 0.5; 3) 1.0; 4) 1.5 cm; 5) $I^2(U)$ of the ion current at $r = 0$; 6, 7) $I^2(U)$ obtained in displacement of the axis of potentials. I^2 , A².

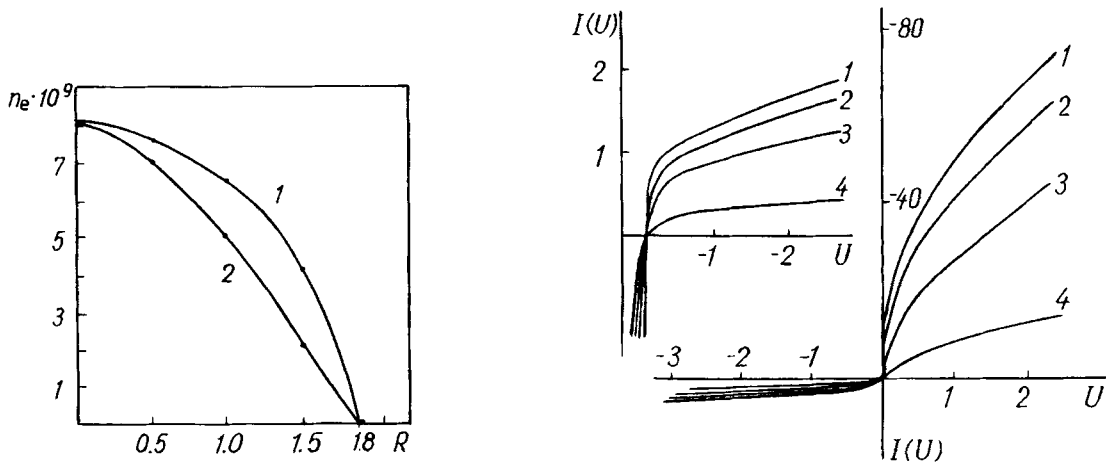


Fig. 3. Profile of the electrons in the active discharge phase: 1) $n_e(R)$; 2) Bessel function. $n_e(R)$, cm⁻³; R , cm.

Fig. 4. Radial dependence of the VAC in a disintegrating plasma: 1) $r = 0$; 2) 0.5; 3) 1.0; 4) 1.5 cm. I , μ A.

Determination of the density of the positive ions is a more complicated problem. Thus, according to the OML theory their concentration on the tube axis exceeds 10^{11} cm⁻³, which (as shown below) is a highly overestimated value. In [3], the authors give attention to a similar effect; however the correction formula proposed by them does not allow one to obtain densities that substantially approach the actual value. It might be supposed that the overestimated value is a result of incorrect determination of the axis of potentials (the current's zero), and then in this case it is easy to carry out a test: upon artificial displacement of the axis of potentials the dependence $I^2(U)$ ceases to be a linear function (see curves 6 and 7 in Fig. 2). This, in turn, allows us to propose a prescription for determination of the floating potential.

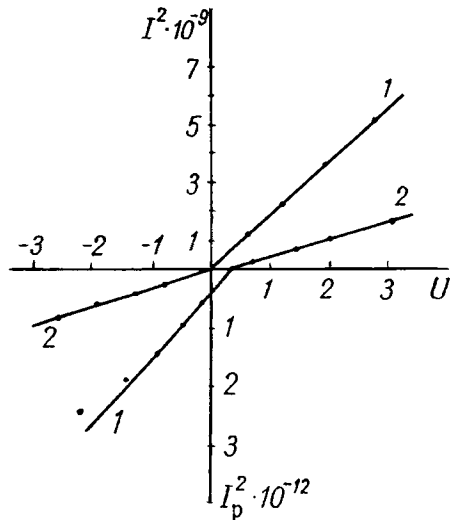


Fig. 5. Plot of $I^2(U)$ on the tube axis for delays of: 1) 40 μsec ; 2) 150.

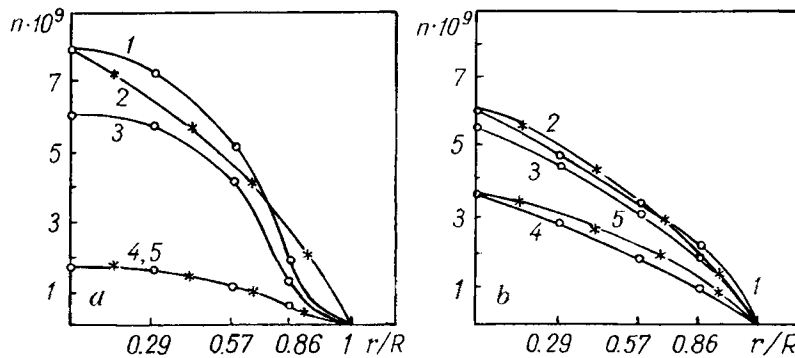


Fig. 6. Concentration profiles of the electrons and positive and negative ions for delays of: a) 40 μsec ; b) 150 (the electron density is increased tenfold); 1) n_p ; 2) Bessel function for the positive ions; 3) n ; 4) n_e ; 5) Bessel function for electrons. $[n(R), n_p(R), n_e(R)] \cdot 10^9, \text{cm}^{-3}$; R, r, cm .

According to the OML theory, the linearity of $I^2(U)$ is a consequence of a Maxwell velocity distribution for particles.

Figure 4 shows the radial dependence of VAC measured by the cylindrical probe with a length of 0.35 cm and a radius of 0.005 cm 40 μsec after the discharge pulse had ceased. As is seen, the current of negative particles is much higher than that of positive ions, but it also has no saturation region. Figure 5 shows plots of $I^2(U)$ on the tube axis for time delays of 40 and 150 μsec . The densities of the electrons and the positive ions were determined from the slope of $I^2(U)$, and the concentrations of the negative ions were found from the condition of quasineutrality of the plasma. Their absolute values were:

$t, \mu\text{sec}$	n_e	n	n_p, cm^{-3}
40	$1.86 \cdot 10^9$	$6.1 \cdot 10^9$	$7.96 \cdot 10^9$
150	$3.6 \cdot 10^8$	$5.5 \cdot 10^9$	$6.0 \cdot 10^9$

The electron temperature was determined by taking the logarithm of $I''(U)$; its value reached 330 K already at the 40th μsec of decay. The temperature of the positive ions determined from the intersection of the curve $I^2(U)$ with the axis of potentials has a significantly overestimated value. Thus, proceeding from the graphs in Fig. 5, we find $T_e + T_p = 0.2 \text{ eV}$, and then the temperature of the positive ions is 0.17 eV. We suppose that a low value of the electron temperature is possible due to efficient interaction of the electrons

with rotational and vibrational levels of oxygen molecules and due to diffusional cooling of the electrons [4]. The temperature of the ions is determined by the energy contribution of the discharge; here owing to the equal masses of the neutral molecules and the ions the latter transfer energy as a result of 1-2 collisions, and consequently, the ions have the same temperature as the gas. Calculation of the energy contribution confirms this supposition. Temperature estimates from the characteristic decay time of the concentrations lead us to the same conclusion.

Figure 6 presents radial profiles of the densities of the charged particles for delay times of 40 and 150 μsec . For earlier delays the ion profiles have a more pronounced convex form than a Bessel distribution. This picture correlates with Fig. 3. Since the characteristic diffusion time of the ions is 600 μsec , the ion profile cannot change strongly in 40–50 μsec , and by virtue of fulfillment of the quasineutrality condition it must repeat the electron profile. Consequently, the ion concentration could also not decrease substantially; moreover, in 150 μsec of decay the density of the positive ions falls only 25%, and therefore in the active discharge phase it must approach 10^{10} cm^{-3} . As regards the negative ions, they are blocked by the electron field [5] and their concentration remains practically constant in the electron stage of decay. Thus, the overestimated value of the density of the positive ions should be related to collisions that occur in the near-probe layer. Indeed, the estimates of λ from the mobilities under the given conditions are 0.014 and 0.01 cm for the negative and positive ions, respectively. The thickness h [6] of the layer of negative space charge in the active phase of the discharge is of the order of several Debye radii ($d = 1.2 \cdot 10^{-2} \text{ cm}$), while for the positive ions the layer increases significantly: its value is determined by the degree of electronegativity $\alpha = n/n_e$ and the temperature ratio T_e/T_p . As is seen from these estimates, $h \gg \lambda_p$ and, consequently, a more complicated theory should be used to describe the current toward an attracting probe. We will try to construct one. According to the estimates obtained, the positive ions are transferred to the probe in a drift mode, and then the current toward the probe is

$$I_p(U) = en_p h_p ES. \quad (1)$$

We determine the size of the layer from the Poisson equation

$$\text{div } E = 4\pi e \left[n_p - n \exp\left(-\frac{eU}{kT_n}\right) - n_e \exp\left(-\frac{eU}{kT_e}\right) \right]. \quad (2)$$

To solve (2), we make a number of assumptions. First, since we determine n_p in the region $eU \gg kT_e$, the terms with $\exp(-eU/kT)$ can be neglected. Second, we use the experimental fact that the current of positive ions toward the probe has the square-root dependence

$$I_p(U) = en_p S \frac{\sqrt{kT_p + eU}}{\sqrt{\pi M_p}}.$$

To simplify the solution of (2), we consider the geometry to be two-dimensional, and then

$$\frac{\partial \frac{eE}{kT_e}}{\partial x} = \frac{(\alpha + 1) I_p \sqrt{\pi M_p}}{eS \sqrt{kT_p + eU}} \frac{4\pi e^2 n_e}{kT_e};$$

under the differential sign the numerator and denominator will be scalar-multiplied by x :

$$\frac{\partial \frac{exE}{kT_e}}{\partial x^2} = \frac{(\alpha + 1) I_p \sqrt{\pi M_p}}{eS \sqrt{kT_e} \sqrt{T_p/T_e + eU/kT_e}}. \quad (3)$$

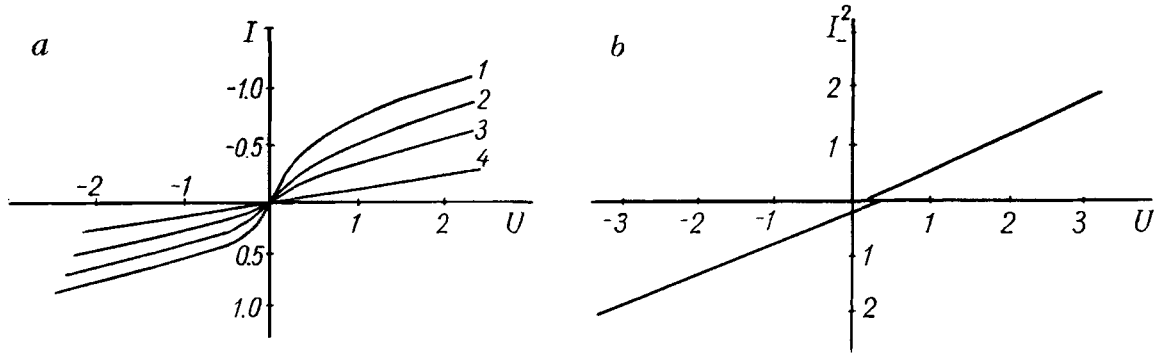


Fig. 7. Radial dependence of the VAC for a delay of 230 μsec (a): 1) $r = 0$; 2) 0.5; 3) 1.0; 4) 1.5 cm and a plot of $I^2(U)$ on the tube axis (b). I , A; $I^2(U)$, μA^2 .

The third assumption is that

$$\frac{e\langle pE \rangle}{kT_e} = \frac{\langle pE \rangle}{kT_e} = \frac{\varepsilon(U) eU}{kT_e} = \eta_{\text{eff}},$$

where the angle brackets indicate the scalar product, and the meaning and the value of $\varepsilon(U)$ are given in [7]. However, this assumption needs more acute substantiation. The energy of a substance in an electromagnetic field contains, in addition to the thermodynamic potentials, the term $DEV/8\pi$ [8]. In the case of charged particles located in an electric field, the elementary work of the field is $dW = NeEdl$; in order to find the mean dipole moment of the charged particles, it should be averaged over the layer size [7]. However, in practice another approach is more suitable. At low particle densities, $D(E) = \varepsilon(E)E$, and the reduced energy is $\eta_{\text{eff}} = \varepsilon(U)eU/(kT)$. Estimates show that in the case of the charged particles η_{eff} is substantially higher than the thermodynamic potentials. Then (3) can be written in the form

$$\frac{\sqrt{1/\gamma + \eta_{\text{eff}}} \partial \eta_{\text{eff}}}{\partial \xi^2} = \frac{2(\alpha + 1)^{3/2}}{\sqrt{\alpha\gamma + 1}}. \quad (4)$$

Here, use was made of the expression for the ion current with allowance for the Bohm number

$$I_p(U) = en_p S \frac{\sqrt{kT_e(1 + \alpha)}}{\sqrt{\pi M_p(1 + \alpha\gamma)}}.$$

Expression (4) is integrated elementarily; the limits of integration with respect to η_{eff} are from 0 to η_{eff} ; for ξ , we neglect the probe radius in the lower limit and integrate between 0 and h/d . As a result, we have

$$\frac{h}{d} = \frac{2 \sqrt[4]{1 + \alpha\gamma} (1/\gamma + \eta_{\text{eff}})^{3/4}}{\sqrt{3} (1 + \alpha)^{3/4}}, \quad (5)$$

i.e., a modified 3/4 law. Using (1) and (5) and also $\varepsilon(U)$, whose value is tabulated in [7], we find the density of the positive ions in the active phase of the discharge – in a wide range of η its value is $n_p = 1.51 \cdot 10^9 \text{ cm}^{-3}$. Since the concentration of the electrons in the active phase is $8.2 \cdot 10^9 \text{ cm}^{-3}$ and the density of the negative ions in the electron stage of the decay remains practically constant at $n = 6.1 \cdot 10^9 \text{ cm}^{-3}$, according to the quasineutrality condition the concentration of the positive ions must be $1.43 \cdot 10^{10} \text{ cm}^{-3}$. As is seen, these values practically coincide. Thus, the size of the layer in an electron-ion plasma is determined by the electron Debye radius; here for the negative-probe layer the 3/4 law still holds; however the reduced potential has a somewhat different meaning, namely, it this is the work of the external field against the induced dipole moment occurring

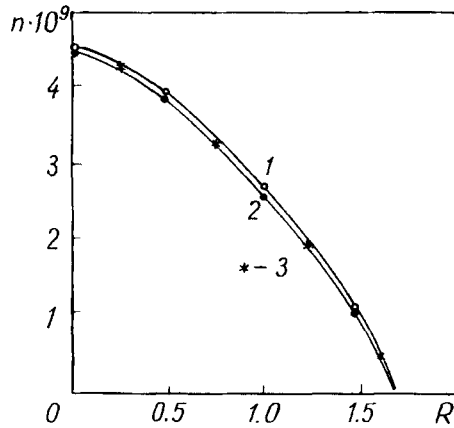


Fig. 8. Concentration profiles of the positive and negative ions for a delay of 230 μsec : 1) n_p ; 2) n ; 3) Bessel function. $[n(R), n_p(R)] \cdot 10^9, \text{cm}^{-3}$; R , cm.

in the layer of space charge. Here, the layer size depends in a complicated manner on the ratio of the electron and ion temperatures and on the degree of electronegativity α . Note that in the absence of electrons in the plasma ($\alpha \rightarrow \infty$) the size of the layer is determined only by η [7].

The profile of the electrons in the initial stage of the decay is close to a Bessel distribution; at later times the profile becomes flatter. As is seen from Fig. 6, the electron concentration in the afterglow stage decreases rapidly and tends to zero at 220–240 μsec [9], and then an ion-ion plasma remains in the space.

Figure 7 presents VAC for a delay of 230 μsec and a plot of $I^2(U)$. The ion temperature determined from the intersection with the axis of potentials is 330–440 K. Note that the same slope of the plots of $I^2(U)$ testifies to fulfillment of the condition of quasineutrality of an ion-ion plasma.

Figure 8 shows radial profiles constructed from $I^2(U)$. It is seen that the distributions of the ions of both signs practically coincide with a Bessel profile. It is noteworthy that, according to the OML theory, the plot of $I^2(U)$ intersects the potential axis at the point where the potential is equal to the particle temperature; in the case of Figs. 2 and 5, the intersection of $I^2(U)$ is reverse. Of course, this order of intersection does not mean that the charged particles possess a negative temperature, it indicates a limited domain of application of the classical OML theory for a plasma of electronegative gases.

Thus, the work provides experimental data on probe-aided measurements in the active phase of the discharge and in the afterglow stage. The overestimation of the density of the positive ions in the active phase of the discharge is explained and a method for its approximate determination in a plasma of electronegative gases is suggested.

NOTATION

$\alpha = n/n_e$, degree of plasma electronegativity; $\gamma = T_e/T_p$, ratio of the electron and ion temperatures; $\epsilon(U)$, dielectric permittivity of the plasma; η , reduced potential; λ_p , mean free path of a positive ion; $\xi = x/d$, reduced coordinate; b_p , mobility of the positive ions; D , electric induction; d , Debye radius of screening; E , electric field; l , particle path in the field E ; e , electron charge; h , size of the near-probe layer; k , Boltzmann constant; M_p , mass of a positive ion; N , gas density; n_e, n_p, n , density of the electrons and the positive and negative ions, respectively; $I_p(U)$, current of positive ions; $I''(U)$, second derivative of the VAC with respect to the potential; R , tube radius; r , current radius; S , probe area; T_e, T_n, T_p , temperature of the electrons and the negative and positive ions, respectively; U , potential applied to the probe; V , volume element; dW , elementary work of the field.

REFERENCES

1. Y. Itikawa, A. Ichimura, K. Onda, K. Sakimoto, and K. Takayanagi, *J. Phys. Chem. Ref. Data*, **18**, No. 1, 23-42 (1989).
2. G. Massey, *Negative Ions* [Russian translation], Moscow (1979).
3. D. Smith, A. G. Dean, and N. G. Adams, *J. Phys. D: Appl. Phys.*, **7**, 1944-1962 (1974).
4. N. S. Kolokolov, A. A. Kudryavtsev, and O. G. Toronov, *Zh. Tekh. Fiz.*, **55**, No. 10, 1920-1927 (1985).
5. V. A. Rozhanskii and L. D. Tsendin, *Collisional Transfer in a Partially Ionized Plasma* [in Russian], Moscow (1988).
6. V. I. Demidov, N. B. Kolokolov, and A. A. Kudryavtsev, *Probe Methods in Low-Temperature Plasma Investigations* [in Russian], Moscow (1996).
7. S. A. Gutsev, *To the Theory of the Near-Probe Layer in an Ion-Ion Plasma* [in Russian], Deposited in VINITI, No. 2956-V97 (*Inzh.-Fiz. Zh.*, **71**, No. 3, 572-573 (1998)).
8. Ya. P. Terletskii, *Statistical Physics* [in Russian], Moscow (1994).
9. S. A. Gutsev, A. A. Kudryavtsev, and V. A. Romanenko, *Zh. Tekh. Fiz.*, **65**, No. 11, 77-85 (1995).